PHILOSOPHICAL TRANSACTIONS B

royalsocietypublishing.org/journal/rstb

Research

Cite this article: Elisha Y, Sagi Y, Klein G, Straussman R, Geiger B. 2019 Cooperativity between stromal cytokines drives the invasive migration of human breast cancer cells. *Phil. Trans. R. Soc. B* **374**: 20180231.
http://dx.doi.org/10.1098/rstb.2018.0231

Accepted: 10 January 2019

One contribution of 13 to a discussion meeting issue 'Forces in cancer: interdisciplinary approaches in tumour mechanobiology'.

Subject Areas:
cellular biology

Keywords:
cell adhesion, invasive migration, epithelial–mesenchymal transition, metastasis, breast cancer

Author for correspondence:
Benjamin Geiger
e-mail: benny.geiger@weizmann.ac.il

†These authors contributed equally to this study.
‡Deceased on 10 December 2016.

Electronic supplementary material is available online at https://dx.doi.org/10.6084/m9.figshare.c.4511636.

THE ROYAL SOCIETY PUBLISHING

Cooperativity between stromal cytokines drives the invasive migration of human breast cancer cells

Yair Elisha[1,†], Yael Sagi[1,†], Georg Klein[2,‡], Ravid Straussman[1] and Benjamin Geiger[1]

[1]Department of Molecular Cell Biology, The Weizmann Institute of Science, Rehovot 7610001, Israel
[2]Department of Microbiology, Tumor and Cell Biology, Karolinska Institute, Stockholm, Sweden

YE, 0000-0002-6348-7894; BG, 0000-0001-8559-6373

The cross-talk between cancer cells and the stromal microenvironment plays a key role in regulating cancer invasion. Here, we employed an *ex vivo* invasion model system for exploring the regulation of breast cancer cells infiltration into a variety of stromal fibroblast monolayers. Our results revealed considerable variability in the stromal induction of invasiveness, with some lines promoting and others blocking invasion. It was shown that conditioned medium (CM), derived from invasion-promoting fibroblasts, can induce epithelial–mesenchymal transition-like process in the cancer cells, and trigger their infiltration into a monolayer of invasion-blocking fibroblasts. To identify the specific invasion-promoting molecules, we analysed the cytokines in stimulatory CM, screened a library of purified cytokines for invasion-promoting activity and tested the effect of specific inhibitors of selected cytokine receptors on the CM-induced invasion. Taken together, these experiments indicated that the invasiveness of BT-474 is induced by the combined action of IL1 and IL6 and that IL1 can induce IL6 secretion by invasion-blocking fibroblasts, thereby triggering cancer cell invasion into the stroma. This unexpected observation suggests that stromal regulation of cancer invasion may involve not only cross-talk between stromal and cancer cells, but also cooperation between different stromal subpopulations.

This article is part of a discussion meeting issue 'Forces in cancer: interdisciplinary approaches in tumour mechanobiology'.

1. Introduction

Recent studies have consistently demonstrated that the cellular properties of cancer are tightly co-regulated by intrinsic, cell-autonomous factors (e.g. expression of oncogenes and tumour suppressors) [1] and external, environmental factors (e.g. cytokines, chemokines and extracellular matrix molecules), which are secreted and processed by diverse non-malignant cells that reside within or in the vicinity of the primary tumour mass [2–5]. The general concept of stromal contribution to cancer cell survival, proliferation and migration, and, consequently, to cancer progression, is widely accepted [2,5]. Less defined is the identity of the specific stromal components that participate in these processes, and the nature of the molecules that mediate them [6,7].

Recent studies demonstrated that multiple cell types residing in the tumour microenvironment, including fibroblasts, endothelial cells, pericytes, adipocytes and diverse immune cells, can affect the fate and behaviour of the cancer cells, both *in vivo* and *ex vivo* [5]. Adipocytes and their secretory products were found to contribute to tumour progression in obesity-associated cancers [8–10]. Endothelial cells and pericytes promote tumour vasculature [11]. Immune cells present in the tumour surroundings were traditionally considered to suppress tumour progression, yet depending on the tissue type and the tumour-specific cellular stimuli, they might be modified in many cases to tumour-promoting

factors, as they secrete inflammatory agents which destroy the tissue and support tumour growth [5].

Fibroblasts, the major cellular component of the cancer stroma, were shown to be quite heterogeneous with regard to their effect on tumour cells. Thus, it was shown that 'normal fibroblasts' (NAFs), which are derived from non-cancerous tissue, may prevent tumour growth, inhibit cell movement and even reverse the invasive phenotype of cancer cells [12–14]. By contrast, 'cancer-associated fibroblasts' (CAFs), which are the prominent cell type in the tumour stroma, commonly promote tumour progression [15]. CAFs lead to invasion by matrix metalloproteinase secretions, and induce angiogenesis by SDF1, cancer growth, invasion and drug resistance [16,17].

Fibroblasts derived from different organs or exposed to different environmental stimuli (e.g. inflammation) display diverse gene expression and tumour promotion profiles [18–20]. Attempts to identify the molecular mediators of stromal stimulation of cancer cells pointed to considerable tumour-specific and stroma-specific variability [2,21–27]. Commonly, specific cytokines (e.g. IL-1, IL-4, IL-6, IL-8, IL-10, TGFβ, TNFα) and chemokines and growth hormones (e.g. SDF1, EGF, platelets-derived growth factor (PDGF), CXCL9, HGF) were shown to be prominent drivers of the stromal stimulation. Some of these were reported to exert their effect on cancer cells by inducing epithelial-to-mesenchymal transition (EMT), thereby increasing the migratory and invasive properties of the cancer cells [14,23,25,28–30], promote angiogenesis [14] or induce extravasation and proliferation at the metastatic site. It is noteworthy that the interaction between cancer and the stroma was found to be a bi-directional process [8]. Cancer cells often generate a supportive microenvironment by producing stroma-modulating growth factors. These include basic fibroblast growth factor, members of the vascular endothelial growth factor family, PDGF, epidermal growth factor receptor ligands, interleukins, colony-stimulating factors, TGFβ and others [4].

In this study, we address the cellular specificity and molecular diversity of the stromal stimulators of cancer invasion using a two-dimensional co-culture system of breast cancer cells (mainly BT-474 cells) and diverse fibroblast lines, some of which were found to be invasion-promoting and others invasion-blocking. We show here that the induction of cancer invasiveness is attributable to secreted stromal factors, rather than to the physical cancer–stromal cell interaction. Our search for the active molecules revealed that BT-474 cancer cell infiltration into the stromal monolayer requires a co-stimulation by IL1 and IL6, each of which was not sufficient for inducing cancer infiltration by itself. The mechanism underlying the synergy between IL1 and IL6, and the significance of this process for cancer metastasis are discussed.

2. Results

(a) Stromal fibroblasts differ in their capacity to modulate cancer cell invasive migration

To explore the effect of stromal fibroblasts on the invasive behaviour of cultured breast cancer cell lines, we have used as our primary model system a two-dimensional co-culture system, in which human breast cancer cells (BT-474 and SKBR3) and diverse fibroblastic cell lines were cultured in a twin-well compartment ('Ibidi insert', see Material and methods) in which the cancer cells and fibroblasts of diverse origins migrate towards each other. Live-cell microscopy of the migrating cancer cells–fibroblasts combinations indicated that the migration of BT-474 or SKBR3 and their infiltration into the fibroblast monolayers were differentially affected by the distinct stromal cell lines. Two of the tested fibroblast lines (HS5 and, to a smaller extent, A26) were readily invaded by the two cancer cell lines (figure 1*a*; electronic supplementary material, Movie S1 and figure S1), whereas all other cell lines tested (CCD1069sk, A6, A9, CCD1090, CAF-GFP, HMF, NAF-GFP and WI-38) formed a clear and stable border with BT-474 (figure 1; electronic supplementary material, Movie S1) or SKBR3 (electronic supplementary material, figure S1 and Movie S2), apparently blocking the invasion by the cancer cells, even following prolonged incubation. The quantification of the infiltration depth confirmed that the cancer cells' penetration into the HS5 or A26 stromal monolayers was considerably deeper than that observed with any of the other stromal lines tested (figure 1*b*).

It is noteworthy that the invasion-promoting properties of HS5 and A26 and invasion-blocking properties of all other tested stromal lines could not be attributed to the specific origins of the respective cell lines (e.g. bone marrow, normal and cancerous tissues, see Material and methods).

Based on these results, we have proceeded with an in-depth characterization of the stromal infiltration properties using BT-474 cells in conjunction with HS5 fibroblast, as the most prominent stromal promoter of infiltration, and with the most prominent infiltration blocker, namely CCD1069sk (for short: CCD1069).

Examination of BT-474 throughout their migration towards the different fibroblast lines revealed notable differences in migration speed and cell shape. As shown in figure 1*c*, the average migration velocity of BT-474 cells, before their physical encounter with HS5 cells, was well over twofold higher than that induced by CCD1069 cells. It is noteworthy that in the absence of stromal cells, BT-474 barely migrated in culture. Moreover, examination of BT-474 cells migrating towards the HS5 fibroblasts revealed characteristic shape changes, manifested by the extension of radial projections and acquisition of star-like shape. These morphological changes are apparent in the electronic supplementary material, Movies S1 (BT-474 cells) and S2 (SKBR3 cells).

The facilitated migration and shape changes, which are apparent in the co-culture system with HS5 fibroblasts prior to the physical encounter between the two cell populations, suggested that the differential invasiveness of the cancer cells into the stromal cell monolayer does not depend on the physical interaction between the two cell populations, and is induced by soluble stromal factors that are released into the medium (see electronic supplementary material, Movies S1 and S2, and quantification of the migration velocity in figure 1*c*).

To directly test the possibility that cell invasion is driven by molecules secreted to the medium by HS5 fibroblasts, we have sparsely plated BT-474 and SKBR3 cells; 3 days later, the culture medium was replaced by a cell-free conditioned medium (CM) derived from HS5 or CCD1069 cells for 2–3 days. Examination of the migratory activity and shape of both cancer cell lines revealed major difference between the effects of HS5 CMs and fresh medium, which were similar

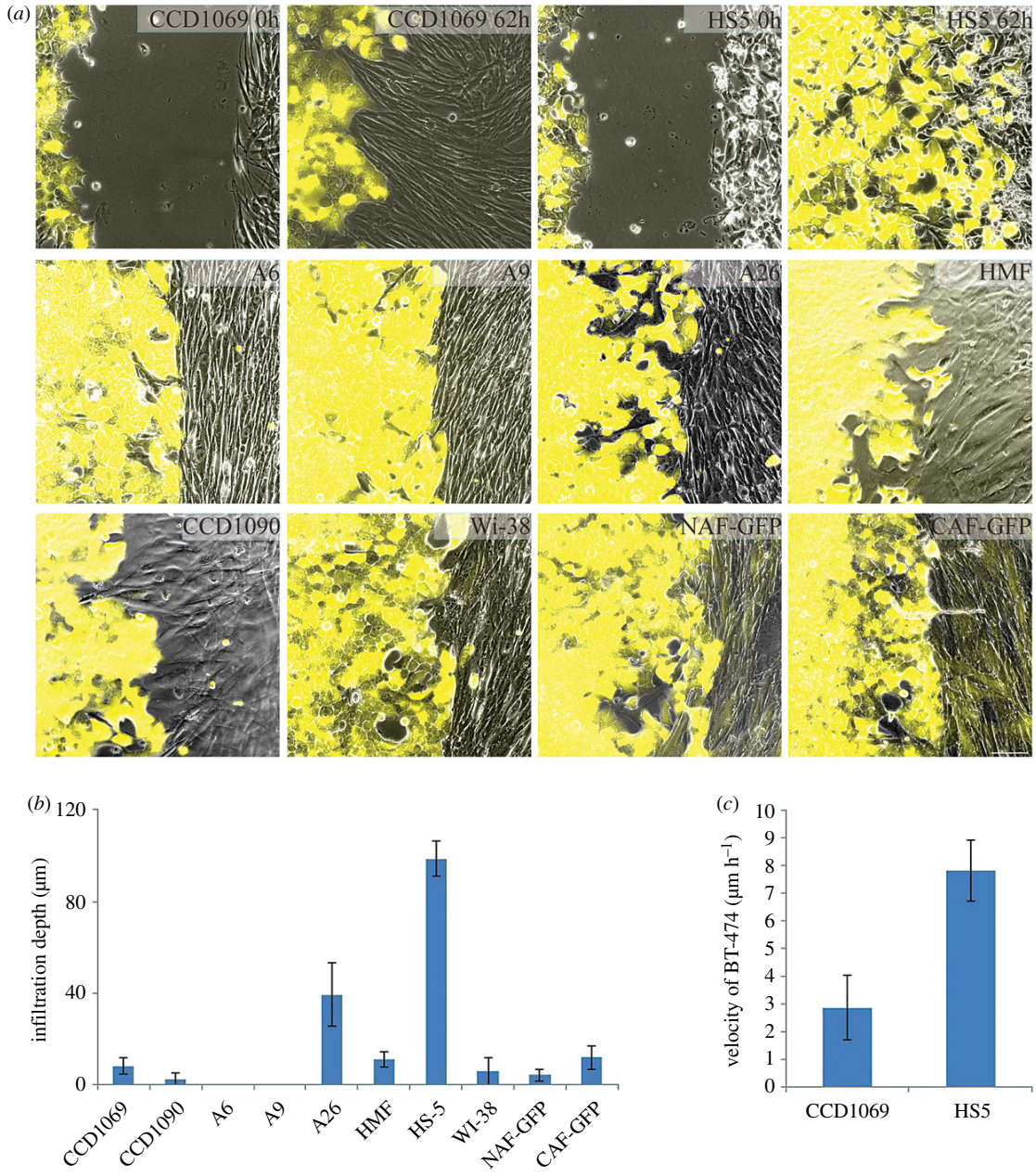

Figure 1. Induction of invasive cancer cell infiltration differs between stromal fibroblasts. (*a*) Various stromal cells (as indicated at the top-right corner of each image) and BT-474 cells were plated separately into parallel compartments of an Ibidi insert. Forty-eight hours later, inserts were removed, medium was added and the cancer and stromal cells were allowed to migrate towards each other. Initial state ($t = 0$) is presented for HS5 and CCD1069 cells. The rest of the images were taken at $t = 62$ h (*a*). (*b*) Quantification of the infiltration of BT-474 cells into the stromal monolayer. (*c*) The initial migration velocity of BT-474 cells in the presence of CCD1069 or HS5 stromal cells. Scale bar, 100 μm.

to those described in figure 1 and in electronic supplementary material, Movie S1 (data not shown).

(b) HS5 conditioned medium can induce infiltration of BT-474 cells into the invasion-blocking CCD1069 cell monolayer

The invasion assay results suggested that the CMs, derived from the invasion-promoting HS5 and A26 cells, contain components that can induce invasive migration, but failed to show whether the invasion-blocking cells (CCD1069) physically interfere with the invasive process. To address this issue, we have plated BT-474 cells and CCD1069 cells in the twin-well device and compared their invasive properties following treatment with CM derived from either the invasion-blocking CCD1069 cells (figure 2*a*, left panels) or from the invasion-promoting HS5 cells (figure 2*a*, right panels). The CM were added either right after lifting the silicon insert, namely initiation of migration (figure 2*a*, upper panels), or 3 days later, following the formation of a clear interface between the cells (figure 2*a*, lower panels). As shown in figure 2*a* and quantified in figure 2*b* (corresponding to the data shown in the lower panels), addition of HS5 CM to the BT-474 cells induced conspicuous invasion into the CCD1069 monolayer, while the addition of CCD1069 CM did not display such activity.

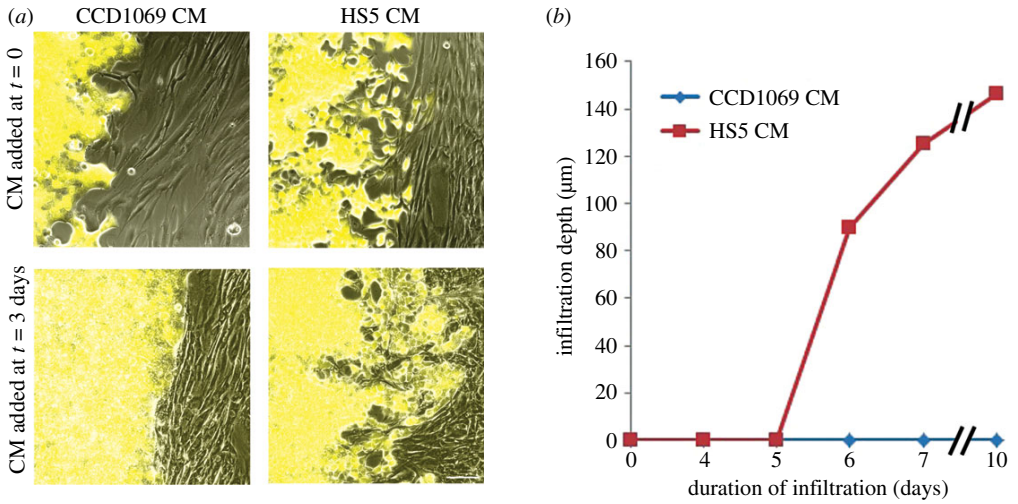

Figure 2. Stromal HS5 CM enables cancer cell infiltration into the blocking stromal fibroblasts CCD1069 monolayer. (*a* upper panels) BT-474 and CCD1069 cells were plated as in figure 1*a* and incubated either with CCD1069 CM (left image) or with HS5 CM (right image), and further incubated for 72 h. Note that cultures supplemented at $t = 0$ with HS5 CM showed extensive invasion of the BT-474 cancer cells into the stromal monolayer, whereas in the presence of CCD1069 CM, the cancer cells failed to penetrate into the stroma. (*a* lower panels) BT-474 and CCD1069 cells were incubated for 72 h and allowed to close the gap between them. Then, the media were replaced by either CCD1069 CM (left image) or HS5 CM (right image) and the cells were further incubated for an additional 3 days, showing that the BT-474 still fails to penetrate to the stromal layer, while the addition of HS5 CM induced strong invasion of the cancer cells into the stroma. (*b*) Quantification of the invasion of BT-474 into the stromal layer shown in *a* (lower panels). Scale bar, 100 μm.

(c) HS5 conditioned medium can induce epithelial-to-mesenchymal transition in BT-474 cells located at the invasive front

Given the EMT-like effects of HS5-derived CM, and the broadly accepted notion that EMT is involved in cancer invasion [13,22,24,27–29], we checked whether BT-474 cells treated with HS5 CM indeed present EMT-like effects, manifested by the loss of cadherin-based cell–cell adhesions and expression of mesenchymal markers such as Snail and Slug. Towards that end, we conducted an infiltration assay with GFP-tagged BT-474 cancer cells and CCD1069 fibroblasts, in the presence of CM, derived from either CCD1069 (top panels of figure 3) or HS5 (lower panels of figure 3) cells. The cells were fixed following 7 days of co-culturing and immunostained for E-cadherin and either Slug (figure 3) or Snail (electronic supplementary material, figure S2). Note that in the presence of HS5 CM, BT-474 cells, primarily those associated with the invading front (bottom panels of figure 3), displayed lower levels of adherens junction-associated E-cadherin, numerous vesicles containing endocytosed E-cadherin and high levels of nuclear Slug and Snail. BT-474 cells located in confluent regions of the culture, far from the interface with the fibroblasts, retained their adherens junctions for a longer period and displayed limited levels of nuclear Slug or Snail.

The addition of CCD1069 CM to the cells (instead of HS5 CM) did not induce any apparent effect on E-cadherin or Snail/Slug localization or expression level either in the invasive front or confluent regions (figure 3; electronic supplementary material, figure S2, upper panels).

(d) IL1 and IL6 are necessary for the HS5 conditioned medium-induced effect on BT-474 cancer infiltration

To identify the components within HS5 CM which promote the invasive process, we have combined three experimental approaches: (i) measurement of the levels of the prominent cytokines in the HS5 CM, which are absent from CCD1069-derived CM [31]; (ii) screening of a secreted molecules library (secretome library) for their 'EMT-like' effect on the morphology of sparsely plated BT-474 and SKBR3 cells; (iii) assessing the effects of cytokine combinations and diverse cytokine inhibitors on BT-474 migration and invasion. Screening of the secretome library was carried out on both BT-474 and SKBR3, and EMT-like effects were noted (in both cell lines) following treatment with OSM, LIF, LTA, IL1α, ILβ and TNFα (data not shown).

Based on the prominence of these cytokines in a broad panel of stromal CMs [31] (namely, abundance in HS5 CM and absence from CCD1069 CM), prime candidates for the effect were IL1α and IL1β. Both cytokines work through the same receptor and exerted essentially the same effect on invasion. It is noteworthy that another stimulator of EMT-like shape changes in BT-474 cells was TNFα; nevertheless, the levels of this cytokine in HS5 CM are rather low and, most likely, do not contribute to the invasive activity induced by HS5 CM (data not shown).

Next, we reproduced the BT-474-CCD1069 invasion assay with pure cytokines (namely, added the cytokines to the cells after a clear interface was formed between them). As shown, the addition of IL1 induced deep invasion of the cancer cells into the stromal monolayer, comparable to that induced by the HS5 CM (figure 4*a*). In order to test whether IL1 is indeed both the essential and sufficient compound in HS5 CM responsible for inducing the invasive migration by the two breast cancer lines, we used the competitive inhibitor of IL1, IL1RA, and found that in its presence, the extent of HS5-induced invasion of BT-474 into the CCD1069 was reduced by more than 90% (figure 4*b*).

IL1 is considered to be an alarm cytokine known to induce the production and secretion of several cytokines, including IL6, IL8, IL10, GM-CSF and SDF1 [32–34]. Among these, IL6 was found to be particularly elevated in

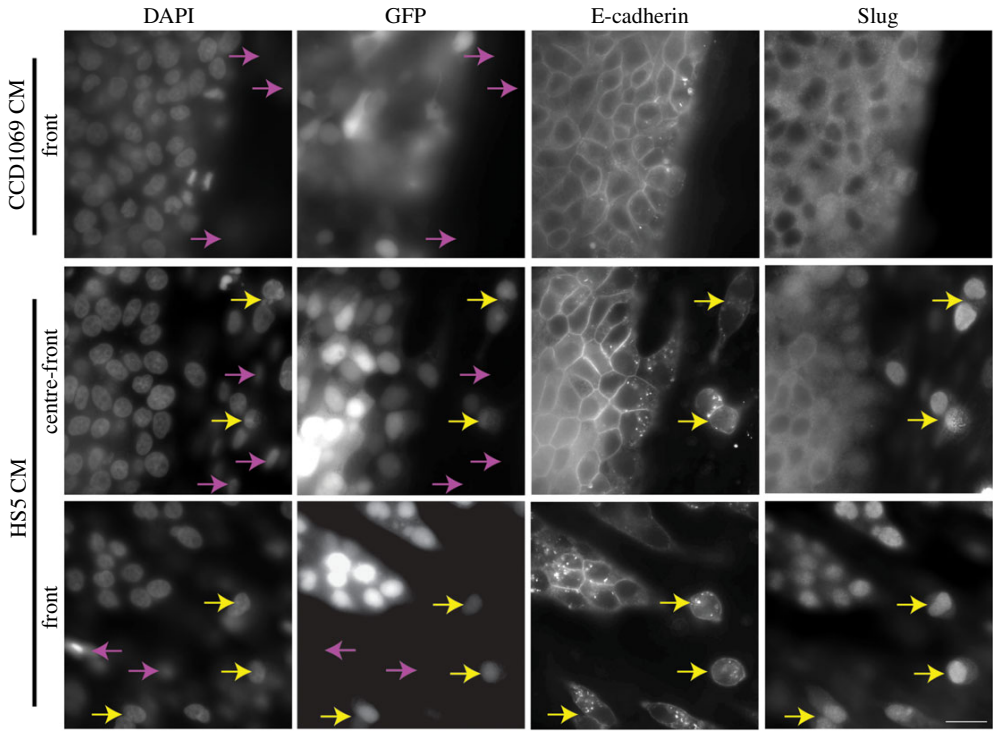

Figure 3. The invasive front of BT-474 interfacing the stromal CCD1069 monolayer, showing EMT-like markers in the invading cells in the presence of HS5 CM. BT-474 and CCD1069 were plated in the invasion assay settings. Medium was added and a clear border between the cells was created after 3 days. CCD1069 or HS5 CMs were added to the cells for an additional 7 days (with medium refresh at day 4). Following 7 days, the cells were fixed and stained for Dapi, Slug and E-cadherin. Yellow arrows point to cancer cells and purple arrows to stroma cells. In the presence of HS5 CM, the invasive front of the cancer cells shows an increase in nuclear Slug and a decrease in the junction-associated E-cadherin. By contrast, BT-474 cells treated with CCD1069 CM show poor infiltration into the stroma, present low nuclear Slug, and largely continuous junctional E-cadherin staining. Scale bar, 20 µm.

HS5 CM [31]. These findings raised the possibility that IL1 and IL6 might be both needed for the induction of invasive migration, and that the apparent effect of IL1 alone might be attributed to the capacity of IL1 to induce IL6 secretion by the (otherwise) invasion blocking CCD1069 cells (figures 4*a*,*b* and 5).

To test this possibility, we added IL6 neutralizing antibodies to the HS5 CM and conducted an invasion assay. This treatment essentially blocked (by approx. 90%) both the HS5- and the IL1-induced infiltration of BT-474 into the stromal monolayer (figure 4*b*), implying that IL6 is essential for stimulation of invasiveness, Interestingly, IL6 by itself, even at very high concentrations, was not sufficient, indicating that both IL1 and IL6 are essential for the induction of cancer infiltration (figure 4*b*).

(e) IL1 induces the secretion of IL6 by the blocking stromal CCD1069 cells, thereby enabling the combined infiltration-promoting effect of the two cytokines

To characterize the interplay between IL1 and IL6, associated with the induction of invasive migration, we have conducted a cell scattering assay in which confluent islands of BT-474 cells were treated with different mixtures of CCD1069 CM and cytokines (figure 5). We deliberately refrained from including live stromal cells in the culture to reduce the complexity of the system (e.g. dynamic cross-talk between the cancer and stromal cells).

Examination of the scattering of BT-474 cells (figure 5*a*) indicated that HS5 CM, which induced a strong invasive behaviour in the cancer cells–stromal cells interface, also triggered conspicuous scattering of the confluent cancer cells. Interestingly, IL1, which induced an EMT-like response in sparse cultures of BT-474 cells, did not scatter the densely plated cells. Similarly, the addition of IL6 to the cells did not induce scattering, yet co-stimulation of the cells by the two cytokines resulted in major scattering that was comparable and often stronger than that caused by HS5 CM. Interestingly, the addition of other IL1-induced 'motogenic cytokines' (IL8, GM-CSF and SDF1) to IL1 itself did not result in cancer cell scattering. The essential role of IL6 in the scattering process induced by the crude HS5 CM is further demonstrated by the capacity of inhibitory IL6 antibodies to suppress the scattering process induced by HS5 CM.

To address the unexpected capacity of IL1 alone to induce invasion in the BT-474-CCD1069 system, we have compared the capacity of CM derived from CCD1069 that were either stimulated by IL1, or cultured in IL1-free medium and supplemented with IL1 just before adding the medium to the cancer cells. As shown in figure 5*a*, the CM obtained from IL1-treated CCD1069 exerted strong scattering effects, while the addition of IL1 to untreated CCD1069 CM had no visible scattering effect. As mentioned above, quantification of IL6 levels clearly indicated that IL1-treated CCD1069 cells secrete IL6 into the medium at levels that exceed those present in HS5 CM, while CM of untreated CCD1069 contains essentially no IL6 (figure 5*b*).

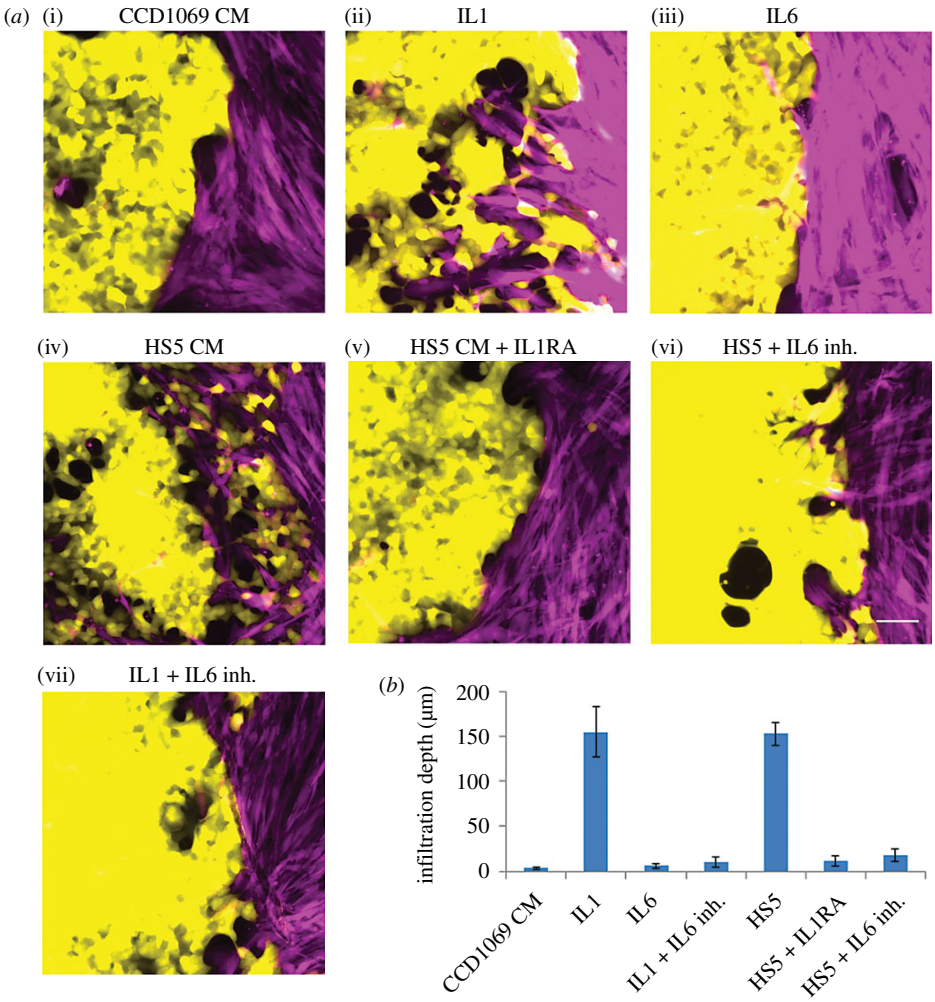

Figure 4. IL1 and IL6 in HS5 CM are both essential for the invasion of BT-474 into CCD1069 stromal cells. (*a*) BT-474 and CCD1069 were plated in the invasion assay settings. Medium was added and the co-cultures were incubated for 3 days, until a clear border between the cells was created. The cultures were further incubated with: (i) CCD1069 CM; (ii) IL1 (IL1α,β 50 ng ml^{-1} each); (iii) IL6 1 μg ml^{-1}; (iv) HS5 CM; (v) HS5 CM + IL1RA (14 μg ml^{-1}); (vi) HS5 CM+ IL6 inh. (a combination of IL6 inhibitors); (vii) IL1 (as above)+IL6 inh. (as above). The cells were then incubated for an additional 4 days, and the infiltration into the stromal monolayer calculated. (*b*) Quantification of cancer cell infiltration into the stromal monolayers. Scale bar, 100 μm.

3. Discussion

In this study, we have used a two-dimensional co-culture system for studying the factors that affect cancer cell infiltration into the surrounding stromal compartment. We found that soluble factors secreted by the fibroblasts were the major inducers of this cancer infiltration. We propose here that this process induced by the HS5 CM is an EMT-like process, which is manifested by massive endocytosis and loss of E-cadherin and upregulation of typical stromal markers including Slug (figure 3) and Snail (electronic supplementary material, figure S2). Interestingly, examination of the migrating cancer cells indicated that the EMT was particularly pronounced in the cancer cells located at the 'invasive front' while confluent BT-474 cells displayed reduced or delayed EMT. This phenomenon has been noticed in other cell types [35–39].

By combining a screening of a secretome library and diverse stromal cell lines for invasive migration of BT-474 and SKBR3 cells, we identified IL1 as potent inducer of BT-474 infiltration. Interestingly, further characterization indicated that IL1 is essential, but not sufficient for inducing cancer infiltration in the two-dimensional culture system. As we show here, IL1 can induce the production of an additional active compound, namely, IL6, that cooperates with IL1 in inducing stromal infiltration. Importantly, neither IL1 nor IL6 were able to trigger the complex process of invasion alone, and only a combination of IL1 and IL6 was able to trigger invasion. It should be mentioned that another cytokine from the secretome library screening, namely TNFα, exhibited invasion-promoting properties similar to those of IL1 (including the induction of IL6 secretion by the invasion-blocking CCD1069 cells). However, its activity was not further investigated, since its levels in the CM of the major invasion-promoting stromal cell line studied here (HS5), were very low.

In this study, we show a strong requirement for the presence of both IL1 and IL6 for induction of invasive migration. IL1 (as well as TNFα) are known to activate the transcription factor NF-κB, while IL6 is a known activator of the STAT3 transcription factor. Cross-talk between these two pathways occurs at several levels: first, activation of the NF-κB pathway induces the expression of several proteins including IL6, which is a potent STAT3 activator. Second, STAT3 was

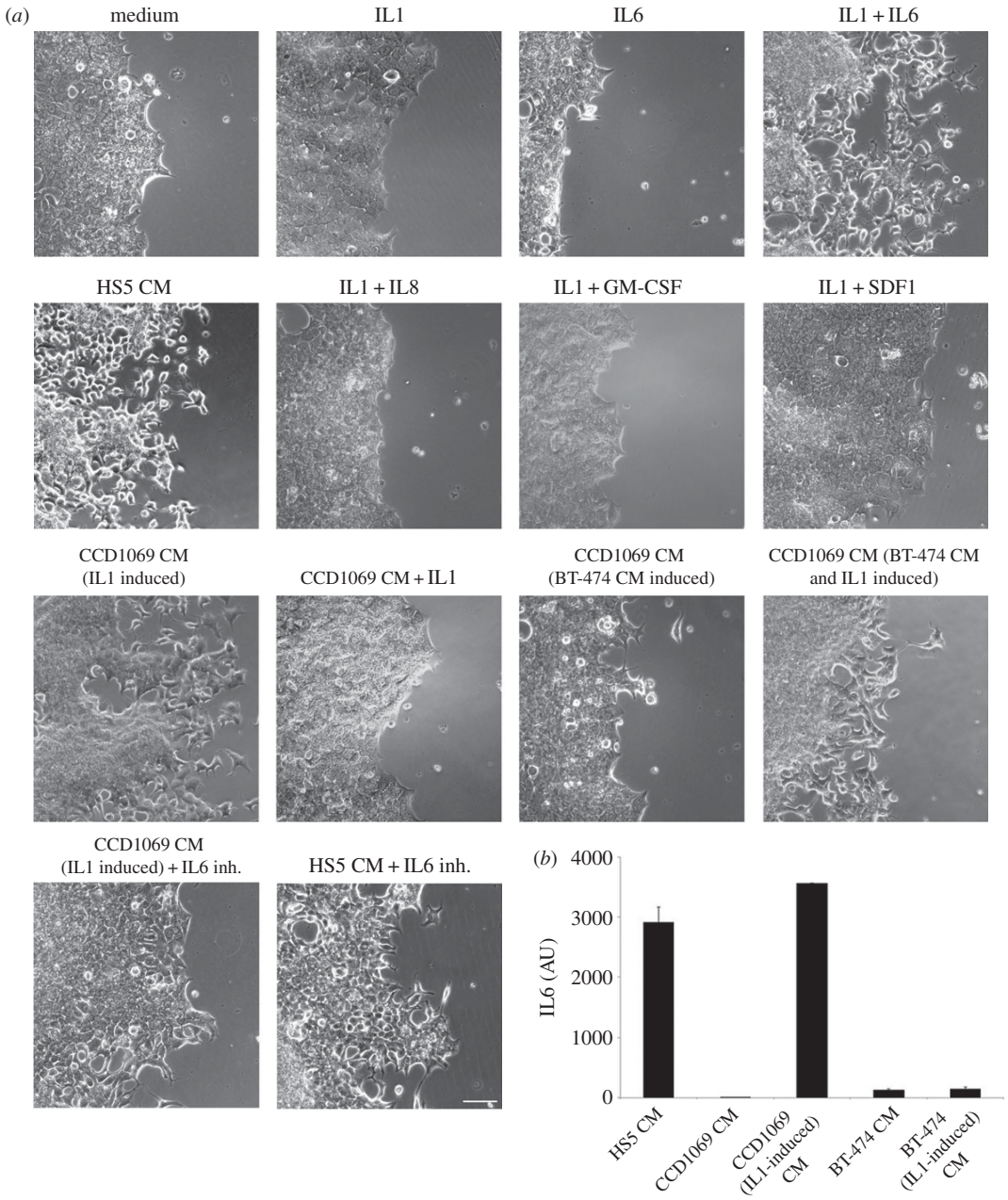

Figure 5. IL1 induces IL6 secretion by CCD1069 cells, thus enabling an EMT-like scattering and invasive migration of BT-474 cells. (*a*) BT-474 cells that were pre-cultured in IBIDI insert (without stromal cells) were further incubated for 72 h in the presence of different CMs or cytokines as indicated. Only HS5 or CCD1069 CMs that were pre-treated with IL1 induced scattering and acquisition of the star-shape of the confluent BT-474 cells. Addition of IL6 inhibitors to either CM blocked the effect. Scale bar, 100 µm. (*b*) Prominents levels of IL6 were detected only in HS5 CM, and in CM of CCD1069 cells that were pre-treated with IL1.

shown to extend the nuclear localization of NF-κB. This was suggested to enable constitutive NF-κB activation by competing with the tightly regulated negative control loop mediated by IκBα [40,41]. Third, STAT3 and NF-κB were shown to physically interact and cooperate at the gene promoter/enhancer [42]; and fourth, the NF-κB-STAT3 complex was shown to bind to unique DNA target sequences to which neither transcription factor can bind on its own [43].

We suggest that the requirement for both IL1 and IL6 for cancer infiltration, as shown here, might be related to this multi-level cross-talk between the STAT3 and NF-κB pathways.

In addition to the synergy between IL1 and IL6 in the invasion process, we demonstrated here cooperativity between the two stromal cell types, HS5 and CCD1069. HS5 is a stromal cell line that originates from the bone marrow and secretes many compounds including IL1 and IL6. CCD1069, on the other hand, is a breast fibroblast cell line which does not secrete IL1 or IL6. In addition, in contrast with HS5, which enables BT-474 and SKBR3 infiltration, CCD1069 blocks stromal invasion by these cells. However, we demonstrated that IL1 alone, added to the CCD1069 line, can induce the secretion of IL6 by these cells (figure 5*b*), essentially converting them from 'invasion blockers' to 'invasion promoters'.

4. Material and methods

(a) Cell lines

BT-474 and SK-BR-3 breast cancer cell lines were obtained from the American Type Culture collection (ATCC catalogue numbers). Fibroblast cell lines used in this study include: HS5, bone marrow-derived (ATCC); CCD1065sk, taken from normal breast tissue removed at mastectomy for metastatic adenocarcinoma (ATCC); CCD1069sk, established from skin taken from normal breast tissue removed at mastectomy for invasive ductal carcinoma (ATCC); foreskin fibroblast cell lines: BJ-hTERT cell lines A, A26, A22, A20, A9, A6, all subcloned from the A cell lines (cloned in Georg Klein's lab).

(b) Antibodies and materials

The following antibodies were used in this study: mouse monoclonal Ab to E-cadherin (BD Biosciences), rabbit monoclonal Ab to Snail (Abcam Co.) and rabbit monoclonal Ab to Slug (Abcam).

Secondary antibodies used in this study: goat anti-mouse IgG conjugated to Cy5, and goat anti-rabbit IgG conjugated to cy3 (Jackson ImmunoResearch Laboratories™, West Grove, PA, USA).

Cytokines: IL1α, IL1β, IL1RA (blocking IL1 receptors), IL6, TNFα, oncostatin M(OSM) (R&D Diagnostics, Minneapolis, MN, USA).

Cytokine inhibitors: IL6-inhibitor (binds to IL-6 itself) (R&D Diagnostics), IL-6 receptor inhibitor (Actemra®/Tocilizumab) (Roche™, Basel, Switzerland).

Tissue culture growth medium: DMEM (Gibco), 10% FCS, pen/strep (Biological industries, Israel), L-Glutamine (Biological industries), Sodium pyruvate (Biological industries); Human Cytokine Array Q1® (RayBiotech™ Norcross, GA, USA)

(c) Conditioned media collection and usage

Cells were grown in tissue culture dishes for 48–72 h, until reaching approximately 80% confluence. The media were collected and filtered with a 0.45 µm filter. The CM was stored at −80°C, thawed and diluted 1 : 1 with fresh medium just before use.

(d) Proliferation assay

Cancer cell lines were plated on 96-well plates. Stromal CMs were added at a 1 : 1 dilution. Four days later, cells were fixed, stained with DAPI and counted with the WiScan Hermes® cell imaging system (Idea Bio-Medical Ltd®, Israel). Twenty fields were acquired from every well, using a 20× air objective. Automatic cell count was performed using WiSoft® software (Idea Bio-Medical Ltd®).

(e) Morphological assays

Cancer cells were plated in a 24-well plate. Sixteen hour later, stromal CMs were added at a 1 : 1 dilution. Twenty-four hours later, pictures were taken using a 20× air objective.

Cancer infiltration. The cells were grown for 48 h in both compartments of a silicon insert, for confluent monolayer (BT-474—5×10^4, SKBR3—2×10^4, CCD1069—2×10^4, A26—4×10^4 cells were plated). The insert was removed, and different CMs were added. The interface between the two cell lines following further incubation was then imaged. The infiltration area was calculated by manually drawing the interface line every single hour, using ImageJ software (National Institutes of Health, USA).

(f) Screening the cancer secrotome library

Cells were plated in a 384-well plate; a day later, the secrotome library including 300 compounds [31] was added to the plate in a final concentration of 50 ng ml^{-1}. Four days later, the cells were fixed. Following cell fixation, cells were counted with the Hermes® cell imaging system (produced by Idea Bio-Medical Ltd, Rehovot). Twenty fields were acquired from every well, using a 20× air objective. Automatic cell count was performed by a software known as 'cell count' also developed by Idea Bio-Medical Ltd. In addition, using a software known as 'cell acquisition', images of the wells were taken and manually analysed for morphological changes.

(g) Immunofluorescence

Cells were fixed and permeabilized with 3% paraformaldehyde (PFA) in PBS, containing 0.5% Triton X-100 for 2 min, then post-fixed with 3% PFA in PBS for 20–30 min and washed three times in PBS.

The samples were blocked with 0.1% BSA and 1% FCS for 30 min and stained with antibodies against E-cadherin, Slug and/or Snail for 1 h. Following three washes with PBS, the samples were stained with fluorescently labelled secondary antibodies.

(h) Fluorescence microscopy and live-cell imaging

Live-cell imaging and sample examination were performed using a DeltaVision Elite® imaging system (GE Healthcare Bio-Sciences, Pittsburgh, PA, USA).

Fluorescent images were acquired with 60×/1.42NA phase contrast objective, using a CoolSnap HQ2 CCD camera® (Roper Scientific, Germany). Time-lapse imaging was carried out at 15 min intervals, and acquired using 10×/0.3NA objective.

(i) Statistical analysis

Statistical analysis of data was expressed as mean ± s.e.m. (shown as error bar) based on at least two independent experiments with multiple samples each.

(j) Infiltration quantification

Different images were acquired at 4–5 days after gap closure in the cancer infiltration assay (see above). All the images were calibrated to the initial starting point. A manual box was drawn to mark the bulk of the non-scattered cells, and computerized segmentation was used for calculation of the percentage of cells in/out the box (which we use as infiltration score).

Data accessibility. This article does not contain any additional data.

Authors' contributions. Y.E., Y.S., B.G., R.S. and G.K. designed the experiments; R.S. provided data on cytokine content of stromal conditioned media; Y.E. and Y.S. performed the experiments; B.G. Y.E. and Y.S. wrote the paper.

Competing interests. We declare we have no competing interests.

Funding. This study was supported by the Israel Science Foundation, grant no. 2749/17 (B.G.).

Acknowledgements. This study was initiated and inspired by the late Georg Klein (1925–2016), a leading cancer biologist, immunologist, a humanist and a dear friend (https://www.nature.com/articles/542296a). Visiting the Weizmann Institute with his wife, Eva, in March 2014, Georg proposed to study, jointly, the 'stromal effects' on invasive cell migration. The results of these experiments were shared with him till his death in 2016. We would like to express our gratitude to members of the Klein team in the Karolinska Institute in Stockholm for their help and cooperation. We would like to thank Barbara Morgenstern for her expert style editing of this article. B.G. is the incumbent of the Erwin Neter Professorial Chair in Cell and Tumor Biology.

References

1. Hazan RB, Kang L, Roe S, Borgen PI, Rimm DL. 1997 Vinculin is associated with the E-cadherin adhesion complex. *J. Biol. Chem.* **272**, 32 448–32 453. (doi:10.1074/jbc.272.51.32448)
2. Gupta GP, Massague J. 2006 Cancer metastasis: building a framework. *Cell* **127**, 679–695. (doi:10.1016/j.cell.2006.11.001)
3. McAllister SS, Weinberg RA. 2014 The tumour-induced systemic environment as a critical regulator of cancer progression and metastasis. *Nat. Cell Biol.* **16**, 717–727. (doi:10.1038/ncb3015).
4. Mueller MM, Fusenig NE. 2004 Friends or foes—bipolar effects of the tumour stroma in cancer. *Nat. Rev. Cancer* **4**, 839–849. (doi:10.1038/nrc1477)
5. Joyce JA, Pollard JW. 2009 Microenvironmental regulation of metastasis. *Nat. Rev. Cancer* **9**, 239–252. (doi:10.1038/nrc2618)
6. Flaberg E, Guven H, Savchenko A, Pavlova T, Kashuba V, Szekely L, Klein G. 2012 The architecture of fibroblast monolayers of different origin differentially influences tumor cell growth. *Int. J. Cancer* **131**, 2274–2283. (doi:10.1002/ijc.27521)
7. Flaberg E *et al.* 2011 High-throughput live-cell imaging reveals differential inhibition of tumor cell proliferation by human fibroblasts. *Int. J. Cancer* **128**, 2793–2802. (doi:10.1002/ijc.25612)
8. Quail DF, Joyce JA. 2013 Microenvironmental regulation of tumor progression and metastasis. *Nat. Med.* **19**, 1423–1437. (doi:10.1038/nm.3394)
9. Nieman KM, Romero IL, Van Houten B, Lengyel E. 2013 Adipose tissue and adipocytes support tumorigenesis and metastasis. *Biochim. Biophys. Acta* **1831**, 1533–1541. (doi:10.1016/j.bbalip.2013.02.010)
10. Park J, Euhus DM, Scherer PE. 2011 Paracrine and endocrine effects of adipose tissue on cancer development and progression. *Endocr. Rev.* **32**, 550–570. (doi:10.1210/er.2010-0030)
11. Hanahan D, Weinberg RA. 2011 Hallmarks of cancer: the next generation. *Cell* **144**, 646–674. (doi:10.1016/j.cell.2011.02.013)
12. Hayashi N, Cunha GR. 1991 Mesenchyme-induced changes in the neoplastic characteristics of the Dunning prostatic adenocarcinoma. *Cancer Res.* **51**, 4924–4930.
13. Olumi AF, Grossfeld GD, Hayward SW, Carroll PR, Tlsty TD, Cunha GR. 1999 Carcinoma-associated fibroblasts direct tumor progression of initiated human prostatic epithelium. *Cancer Res.* **59**, 5002–5011. (doi:10.1186/bcr138)
14. Alkasalias T, Flaberg E, Kashuba V, Alexeyenko A, Pavlova T, Savchenko A, Szekely L, Klein G, Guven H. 2014 Inhibition of tumor cell proliferation and motility by fibroblasts is both contact and soluble factor dependent. *Proc. Natl Acad. Sci. USA* **111**, 17 188–17 193. (doi:10.1073/pnas.1419554111)
15. Micke P, Ostman A. 2004 Tumour-stroma interaction: cancer-associated fibroblasts as novel targets in anti-cancer therapy? *Lung Cancer* **45**(Suppl. 2), S163–S175. (doi:10.1016/j.lungcan.2004.07.977)
16. Kalluri R. 2016 The biology and function of fibroblasts in cancer. *Nat. Rev. Cancer* **16**, 582–598. (doi:10.1038/nrc.2016.73)
17. Scherz-Shouval R *et al.* 2014 The reprogramming of tumor stroma by HSF1 is a potent enabler of malignancy. *Cell* **158**, 564–578. (doi:10.1016/j.cell.2014.05.045)
18. Direkze NC, Hodivala-Dilke K, Jeffery R, Hunt T, Poulsom R, Oukrif D, Alison MR, Wright NA. 2004 Bone marrow contribution to tumor-associated myofibroblasts and fibroblasts. *Cancer Res.* **64**, 8492–8495. (doi:10.1158/0008-5472.can-04-1708)
19. Quante M *et al.* 2011 Bone marrow-derived myofibroblasts contribute to the mesenchymal stem cell niche and promote tumor growth. *Cancer Cell* **19**, 257–272. (doi:10.1016/j.ccr.2011.01.020)
20. Rinn JL, Bondre C, Gladstone HB, Brown PO, Chang HY. 2006 Anatomic demarcation by positional variation in fibroblast gene expression programs. *PLoS Genet.* **2**, e119. (doi:10.1371/journal.pgen.0020119)
21. Thiery JP, Acloque H, Huang RY, Nieto MA. 2009 Epithelial–mesenchymal transitions in development and disease. *Cell* **139**, 871–890. (doi:10.1016/j.cell.2009.11.007)
22. Nicolini A, Carpi A, Rossi G. 2006 Cytokines in breast cancer. *Cytokine Growth Factor Rev.* **17**, 325–337. (doi:10.1016/j.cytogfr.2006.07.002)
23. Xie G *et al.* 2012 IL-6-induced epithelial-mesenchymal transition promotes the generation of breast cancer stem-like cells analogous to mammosphere cultures. *Int. J. Oncol.* **40**, 1171–1179. (doi:10.3892/ijo.2011.1275)
24. Zhao Z *et al.* 2014 Metformin inhibits the IL-6-induced epithelial-mesenchymal transition and lung adenocarcinoma growth and metastasis. *PLoS ONE* **9**, e95884. (doi:10.1371/journal.pone.0095884)
25. Palena C, Hamilton DH, Fernando RI. 2012 Influence of IL-8 on the epithelial-mesenchymal transition and the tumor microenvironment. *Future Oncol.* **8**, 713–722. (doi:10.2217/fon.12.59)
26. Li Y, Wang L, Pappan L, Galliher-Beckley A, Shi J. 2012 IL-1β promotes stemness and invasiveness of colon cancer cells through Zeb1 activation. *Mol. Cancer* **11**, 87. (doi:10.1186/1476-4598-11-87)
27. Ma L *et al.* 2012 Epidermal growth factor (EGF) and interleukin (IL)-1β synergistically promote ERK1/2-mediated invasive breast ductal cancer cell migration and invasion. *Mol. Cancer* **11**, 79. (doi:10.1186/1476-4598-11-79)
28. Yadav A, Kumar B, Datta J, Teknos TN, Kumar P. 2011 IL-6 promotes head and neck tumor metastasis by inducing epithelial-mesenchymal transition via the JAK-STAT3-SNAIL signaling pathway. *Mol. Cancer Res.* **9**, 1658–1667. (doi:10.1158/1541-7786.mcr-11-0271)
29. Fernando RI, Castillo MD, Litzinger M, Hamilton DH, Palena C. 2011 IL-8 signaling plays a critical role in the epithelial-mesenchymal transition of human carcinoma cells. *Cancer Res.* **71**, 5296–5306. (doi:10.1158/0008-5472.can-11-0156)
30. Yu Y, Xiao CH, Tan LD, Wang QS, Li XQ, Feng YM. 2014 Cancer-associated fibroblasts induce epithelial-mesenchymal transition of breast cancer cells through paracrine TGF-β signalling. *Br. J. Cancer* **110**, 724–732. (doi:10.1038/bjc.2013.768)
31. Straussman R *et al.* 2012 Tumour micro-environment elicits innate resistance to RAF inhibitors through HGF secretion. *Nature* **487**, 500–504. (doi:10.1038/nature11183)
32. Pang G, Couch L, Batey R, Clancy R, Cripps A. 1994 GM-CSF, IL-1α, IL-1β, IL-6, IL-8, IL-10, ICAM-1 and VCAM-1 gene expression and cytokine production in human duodenal fibroblasts stimulated with lipopolysaccharide, IL-1α and TNF-α. *Clin. Exp. Immunol.* **96**, 437–443. (doi:10.1111/j.1365-2249.1994.tb06048.x)
33. Voronov E *et al.* 2013 Unique versus redundant functions of IL-1α and IL-1β in the tumor microenvironment. *Front. Immunol.* **4**, 177. (doi:10.3389/fimmu.2013.00177)
34. Apte RN, Voronov E. 2008 Is interleukin-1 a good or bad 'guy' in tumor immunobiology and immunotherapy? *Immunol. Rev.* **222**, 222–241. (doi:10.1111/j.1600-065X.2008.00615.x)
35. Cichon MA, Nelson CM, Radisky DC. 2015 Regulation of epithelial-mesenchymal transition in breast cancer cells by cell contact and adhesion. *Cancer Inform.* **14**, 1–13. (doi:10.4137/cin.s18965)
36. Sharif GM, Wellstein A. 2015 Cell density regulates cancer metastasis via the Hippo pathway. *Future Oncol.* **11**, 3253–3260. (doi:10.2217/fon.15.268)
37. Sarrio D, Rodriguez-Pinilla SM, Hardisson D, Cano A, Moreno-Bueno G, Palacios J. 2008 Epithelial–mesenchymal transition in breast cancer relates to

the basal-like phenotype. *Cancer Res.* **68**, 989–997. (doi:10.1158/0008-5472.can-07-2017)

38. De Wever O, Pauwels P, De Craene B, Sabbah M, Emami S, Redeuilh G, Gespach C, Bracke M, Berx G. 2008 Molecular and pathological signatures of epithelial–mesenchymal transitions at the cancer invasion front. *Histochem. Cell Biol.* **130**, 481–494. (doi:10.1007/s00418-008-0464-1)
39. Elisha Y, Kalchenko V, Kuznetsov Y, Geiger B. 2018 Dual role of E-cadherin in the regulation of invasive collective migration of mammary carcinoma cells. *Sci. Rep.* **8**, 4986. (doi:10.1038/s41598-018-22940-3)
40. Hennessy BT *et al.* 2009 Characterization of a naturally occurring breast cancer subset enriched in epithelial-to-mesenchymal transition and stem cell characteristics. *Cancer Res.* **69**, 4116–4124. (doi:10.1158/0008-5472.can-08-3441)
41. Chen L, Fischle W, Verdin E, Greene WC. 2001 Duration of nuclear NF-κB action regulated by reversible acetylation. *Science* **293**, 1653–1657. (doi:10.1126/science.1062374)
42. Yang J, Liao X, Agarwal MK, Barnes L, Auron PE, Stark GR. 2007 Unphosphorylated STAT3 accumulates in response to IL-6 and activates transcription by binding to NFκB. *Genes Dev.* **21**, 1396–1408. (doi:10.1101/gad.1553707)
43. Hagihara K, Nishikawa T, Sugamata Y, Song J, Isobe T, Taga T, Yoshizaki K. 2005 Essential role of STAT3 in cytokine-driven NF-κB-mediated serum amyloid A gene expression. *Genes Cells* **10**, 1051–1063. (doi:10.1111/j.1365-2443.2005.00900.x)